

A Dense Grid of Reference Iodine Lines for Optical Frequency Calibration in the Range 595–655 nm

S. C. Xu, R. van Dierendonck, W. Hogervorst, and W. Ubachs

Department of Physics and Astronomy, Laser Centre, Vrije Universiteit, De Boelelaan 1081, 1081 HV Amsterdam, The Netherlands

Received November 15, 1999; in revised form February 4, 2000

A dense grid of reference lines in the hyperfine structure of the $B-X$ transitions of molecular iodine ($^{127}\text{I}_2$) is presented. Frequencies of 481 t -hyperfine components in 15 vibrational bands covering the wavelength range 595–655 nm were determined with an absolute accuracy of 1.0 MHz (1σ uncertainty). Spectra were obtained by Doppler-free saturation spectroscopy using a cw ring-dye laser of 1-MHz bandwidth. Center-of-gravity frequencies of rovibronic lines, determined by correcting for the calculated hyperfine shift, are included separately in a least-squares parametrization for each band. From the obtained molecular constants a prediction is made for all t -hyperfine components of the 15 bands covering 595–655 nm. Hence a dense grid of reference lines of 1 MHz (1σ) absolute accuracy is created, with a line in each interval of 1 cm^{-1} in the entire range. This spectral atlas of about 3400 lines may provide a useful calibration tool in many laboratories. © 2000 Academic Press

1. INTRODUCTION

In high-resolution laser spectroscopy of atoms and molecules there exists a continuous demand for calibration spectra of increased accuracy. Since in many laboratories primary wavelength standards are not readily available, interpolation and comparison with known reference spectra has become a common and useful technique. The work of the Aimé–Cotton group (1, 2) on the Doppler-broadened I_2 spectrum has served this purpose in a large number of spectroscopic studies in the past two decades. However, for many applications this reference standard is not accurate enough. In a previous paper (3) we reported on a dense grid of iodine reference lines in the range 571–596 nm, with an easily identifiable line in each reciprocal centimeter interval with an absolute accuracy of 2 MHz. We note that in the previous study the uncertainties were not explicitly defined; whereas in Ref. (3) we used 2σ for the uncertainty, throughout the present paper we will use 1σ . This standard, based on the $B-X$ system of molecular iodine, is more than an order of magnitude more accurate than previously existed, due to the application of the Doppler-free saturated absorption technique. In the present paper we extend the standard to the range 595–655 nm.

Based on the measurement of transition frequencies of the t -hyperfine component of 481 rotational lines in 15 different bands of the $B-X$ system, a reference standard of components can be constructed, with an accuracy of 1 MHz (taking 1σ as the uncertainty). Our work in the yellow–red range of 571–655 nm extends the work of the Hannover group, where the focus

is on an I_2 -reference standard in the near-infrared at 778–816 nm (4–7).

2. EXPERIMENTAL

The experimental setup, schematically shown in Fig. 1, is essentially the same as the one used for the previous study, and for details we refer to Ref. (3). For the wavelength ranges 595–620 nm the ring-dye laser is operated with Rhodamine-B, whereas for the range 620–655 nm DCM dye is used.

It is noted that no direct wavelength measurements are performed and that our procedures rely on interpolation between I_2 lines that have been calibrated with high accuracy by other groups. For the range 595–655 nm frequencies of a total of 60 hyperfine components in the $B-X$ spectrum of I_2 were determined by Shiner *et al.* (8), Quinn (9), Edwards *et al.* (10), and Sansonetti (11). These lines are all known to within 0.5 MHz (1σ) and some even with much higher accuracy; in the papers usually 2σ uncertainties are given. These 60 lines provide a primary frequency standard for the present experiment.

The measurement procedure of our study is as follows. A measurement session is defined by the period over which a 633-nm ^3He – ^{22}Ne laser can be kept locked to an I_2 -hyperfine component using Lamb-dip stabilization with an I_2 cell inside the He–Ne laser cavity. Also during the full period of a session an external étalon is frequency-locked to the output of the He–Ne laser. For each session the free-spectral range (FSR) of the étalon is determined by interpolating the frequency separation between two of the 60 well-calibrated lines. For this purpose only the frequency separation between the specific I_2 resonance with the nearest étalon marker has to be determined; usually an average over three recordings is taken. The integer number of étalon markers between the two chosen reference

Supplementary data for this article are available on the journal home page (<http://www.academicpress.com/jms>) and as part of the Ohio State University Molecular Spectroscopy Archives (http://msa.lib.ohio-state.edu/jmsa_hp.htm).

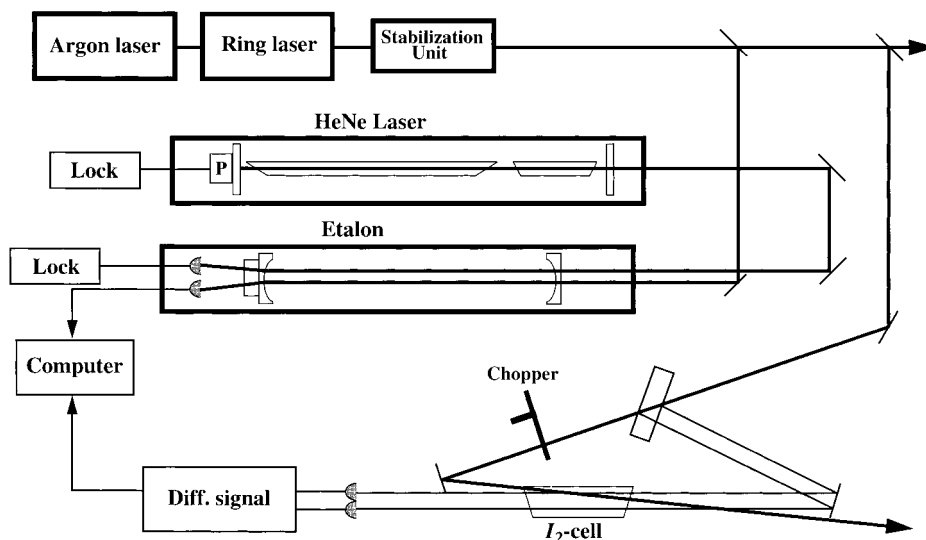


FIG. 1. Scheme of the experimental setup.

lines is known from a first estimate for the FSR: in all sessions a value of 148.956 MHz with a day-to-day variation of less than 0.001 MHz is found, due to the temperature and pressure stabilization of the étalon. In cases when a measurement session lasts several hours repetitive scans of the reference lines are recorded to verify the locking and the value of the FSR. Often a third well-calibrated line, out of the 60 available, is also used for validation. The accuracy in the FSR is, if necessary, improved by choosing pairs of reference lines that are several 100 cm^{-1} apart. Depending on the specific choice of reference lines and their accuracy, the FSR is determined for each session with a precision of typically 0.2–0.5 kHz. At this level of accuracy no effects of dispersion nor of varying penetration depth in the mirror coatings were observed over the wavelength range of this study. Finally the data on the newly calibrated lines also provide an additional consistency check, because they can be included in a least-squares fit to the rotational structure (see below).

These procedures in effect connect to the position of each étalon marker an absolute frequency value. The relative measurement of the separation between an étalon marker and one of the 60 primary lines establishes this absolute scale.

Subsequently t -hyperfine components of additional lines are recorded. A typical example of such a spectrum is presented in Fig. 2 for the $P60$ and $R66$ lines in the (7–3) band. The width of an isolated saturation component is 11 MHz. Absolute frequencies of the t components in the hyperfine structure can be determined by fitting the I_2 spectrum as well as the étalon spectrum to a series of Gaussian profiles and by subsequent determination of the fractional separation to the nearest étalon fringe. Again it is noted that these procedures only yield valid results if the locking of the He–Ne laser and the étalon is preserved.

The uncertainty in the frequency of a t component can be calculated from the statistical uncertainty in the measurement (average over three or more recordings), the uncertainty in the value for the FSR, and the uncertainty in the reference line selected. The uncertainty in the FSR is again dependent on the statistical error in the measurements of the reference lines and their listed accuracy. Taking all this into account, a measurement error can be determined for each measured value for the frequency of a hyperfine t -component. For all recorded transitions this error is about 1.0 MHz (1σ).

3. RESULTS AND ANALYSIS

The hyperfine t -components of 481 rotational lines in the B – X system of molecular iodine are measured using saturated

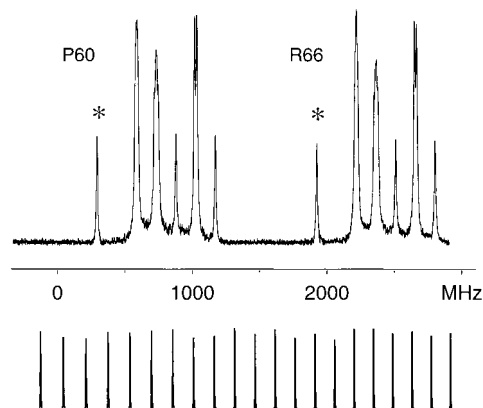


FIG. 2. Simultaneous scan of the $P60$ and $R66$ lines in the B – X (7–3) band of I_2 (upper trace) recorded at 629.42 nm and the fringes of a stabilized étalon (lower trace). The t components are denoted by *.

TABLE 1
Measured Hyperfine t Components for
Various Rotational Lines in the $B-X$ (6, 5)
Band of I_2

Line	Frequency	Δ_{hyp}	$\Delta_{\text{o-c}}$
P17	461330472.5	487.7	0.1
P19	461307691.0	487.8	0.8
P21	461282806.7	488.0	-0.2
P30	461144826.3	488.2	-0.6
P32	461108385.2	488.3	1.5
P34	461069837.4	488.3	-0.1
P36	461029187.1	488.3	-0.9
P68	460092291.7	488.5	-0.9
P72	459937183.1a	488.5	0.0
P78	459688641.7	488.5	-0.4
P100	458613882.7a	488.5	0.4
P101	458558911.2	488.5	1.0
P106	458276044.6	488.5	-0.2
P110	458040135.0a	488.5	-0.2
R17	461389173.1	487.6	0.5
R19	461373096.6	487.8	0.1
R34	461185508.1	488.3	-1.2
R41	461057463.5a	488.4	0.2
R42	461037065.1	488.4	0.3
R46	460950202.2	488.4	-0.6
R74	460105689.2	488.5	-0.2
R85	459660344.7	488.5	-0.4

Note. Δ_{hyp} represents the calculated shift of the t -component from the center-of-gravity of the rovibrational transition. $\Delta_{\text{o-c}}$ represents the deviation of the center-of-gravity from the fitted value. All values in MHz.

^a From Ref. (11).

absorption spectroscopy. The lines belong to 15 vibrational bands: (6-5), (5-4), (6-4), (7-4), (8-4), (7-3), (9-4), (10-4), (9-3), (10-3), (11-3), (12-3), (11-2), (12-2), and (13-2). These bands have the largest Franck-Condon factor and are hence most easily detected in the wavelength range that they cover. The results of these measurements are listed band by band in Tables 1-15. Uncertainties in the frequency positions are not listed separately but they are all within 1 MHz (1σ).

For an analysis of center-of-gravity frequencies and the rotational structure of the bands first the hyperfine structure in the ground and excited states must be addressed. At the level of accuracy of the present analysis only the two most important terms in the hyperfine Hamiltonian have to be included (12):

$$H_{\text{hf}} = eQq \cdot H_{\text{EQ}} + C \cdot H_{\text{SR}}. \quad [1]$$

Here $eQq \cdot H_{\text{EQ}}$ represents the electric quadrupole term and $C \cdot H_{\text{SR}}$ the spin-rotation term. The spin-spin hyperfine interaction is neglected. The two terms of Eq. [1] are sufficient to represent the separation of $F = J$ hyperfine components with respect to the center-of-gravity at the 0.2 MHz level when $\Delta J = \pm 2$ contributions are included in the diagonalization of the hyperfine matrix. In our previous paper (3) we used expressions for the differences between hyperfine constants in ground and excited states ΔeQq and ΔC and assumed $eQq_x = -2452.6$ MHz (13), independent of ν and J . Especially for $\nu'' = 4$ and 5, used in the present study, this simplification gives deviations

TABLE 2
Data for the (5, 4) Band

Line	Frequency	Δ_{hyp}	$\Delta_{\text{o-c}}$
P18	464079298.9	488.2	-1.2
P24	464001809.5	488.6	-0.8
P27	463956012.9	488.6	0.7
P33	463850304.8	488.8	0.6
P36	463790392.4	488.8	0.3
P77	462499012.8a	489.0	-0.4
P78	462456486.0	489.0	-0.4
P80	462369851.9	489.0	-0.3
P82	462281110.0	489.0	0.0
P83	462235947.9	489.0	-0.2
P85	462144041.6	489.0	-0.2
P87	462050024.4	489.0	-0.5
P88	462002224.9	489.0	0.4
P90	461905039.5	489.0	0.1
P91	461855654.7	489.0	0.4
P92	461805740.8	489.0	0.1
P93	461755298.4	489.0	0.0
P95	461652827.3	489.0	0.2
P103	461221763.6	489.0	0.3
R10	464188802.6	486.5	-0.3
R16	464156624.1	488.0	-0.6
R20	464124724.8	488.4	0.0
R28	464035838.7	488.7	-0.1
R37	463895836.8	488.8	0.9
R43	463778949.0	488.8	1.1
R87	462344193.3	489.0	-0.6
R92	462116580.6	489.0	-0.1
R94	462021829.3a	489.0	0.1
R95	461973658.9	489.0	0.3
R96	461924958.9	489.0	1.0
R101	461673497.5	489.0	0.8
R103	461569195.4	489.0	-0.0
R106	461408756.3	489.0	-0.3
R109	461243529.5	489.0	0.1
R112	461073507.7	489.0	-0.6

^a From Ref. (11).

significant on the level of accuracy desired in the present analysis.

Hence an improved treatment of the hyperfine structure is invoked, based on recent work of the Hannover group (4-7).

TABLE 3
Data for the (6, 4) Band

Line	Frequency	Δ_{hyp}	$\Delta_{\text{o-c}}$
P16	467586067.2	487.6	0.3
P19	467552302.4	487.8	0.5
P22	467513747.0	488.0	0.3
P24	467485382.2	488.1	0.8
P33	467331378.2	488.3	-0.3
P39	467204733.9	488.3	-1.0
P50	466922692.4	488.4	0.0
P54	466804117.4	488.4	-0.4
P64	466470265.8	488.5	-0.6
P77	465956214.6	488.5	0.6
P79	465869084.2	488.5	1.0
P82	465734359.3	488.5	1.0
P84	465641854.9	488.5	0.6
P87	465499063.8	488.5	-0.5
P89	465401180.2 ^a	488.5	0.4
P91	465301140.8	488.5	-0.3
P93	465198946.1	488.5	-0.8
P94	465147040.8	488.5	-0.3
P99	464879417.5	488.5	-0.5
P100	464824273.2	488.5	-0.2
P102	464712363.2	488.5	0.3
P103	464655596.4	488.5	-0.2
P104	464598289.6	488.5	0.2
P105	464540441.0	488.5	-0.1
P108	464363647.9	488.5	0.5
P109	464303632.6	488.5	-0.1
P111	464181976.0	488.5	-0.9
P112	464120335.9	488.5	0.5
P113	464058151.2	488.5	0.0
R36	467392823.4	488.3	-0.5
R56	466930868.3 ^a	488.4	0.3
R59	466843133.7	488.4	0.5
R62	466750579.8	488.4	-0.2
R65	466653204.7	488.4	-0.5
R66	466619674.3	488.4	-0.7
R72	466407228.6	488.5	-0.6
R75	466293758.5	488.5	-0.7
R77	466215427.0	488.5	1.0
R79	466134942.7	488.5	0.5
R88	465746120.2	488.5	0.2
R95	465413505.6	488.5	-0.4
R107	464781655.8	488.5	0.4

^a From Ref. (11).

TABLE 4
Data for the (7, 4) Band

Line	Frequency	Δ_{hyp}	$\Delta_{\text{o-c}}$
P25	470904715.9	487.6	1.0
P31	470801981.1	487.8	0.2
P33	470763394.4	487.8	0.4
P39	470634600.9	487.8	0.3
P47	470432448.1	487.9	1.1
P57	470130797.5	487.9	1.3
P60	470029681.7	488.0	0.8
P64	469887228.5	488.0	0.4
P65	469850251.4 ^a	488.0	0.3
P69	469696884.6	488.0	-0.5
P72	469576125.9	488.0	-0.1
P75	469450447.1	488.0	-0.5
P80	469230042.3	488.0	0.0
P83	469091227.1	488.0	-0.8
P89	468798794.8	488.0	-0.2
P91	468696926.5	488.0	0.2
P94	468540002.3	488.0	0.3
P95	468486594.3 ^a	488.0	0.1
P96	468432636.4	488.0	0.1
P98	468323069.2	488.0	-0.1
P102	468097325.9	488.0	0.2
P107	467802737.7	488.0	0.5
P117	467172101.0	488.0	0.9
P118	467105990.6	488.0	0.9
R37	470804663.5	487.8	-0.3
R39	470766455.5 ^d	246.4	-0.0
R45	470637814.0	487.9	1.2
R53	470436131.0	487.9	0.5
R55	470380262.5	487.9	0.6
R61	470199567.7	487.9	0.4
R63	470134970.2	487.9	0.3
R66	470033977.1	488.0	-0.1
R70	469891668.6	488.0	0.2
R75	469701472.3	488.0	-0.3
R78	469580782.7	488.0	-0.3
R81	469455158.9	488.0	-0.4
R89	469096006.7	488.0	-1.4
R95	468803546.9	488.0	-0.5
R100	468544675.3	488.0	0.0
R102	468437262.9	488.0	0.1
R103	468382727.4	488.0	-0.4
R108	468101757.8	488.0	-0.2
R113	467806942.7	488.0	-0.2
R119	467434849.0	488.0	-0.1
R121	467306369.1	488.0	-0.4
R123	467175661.8	488.0	-0.6

^a From Ref. (11).

^d From Ref. (10), "r"-component measured.

TABLE 5
Data for the (8, 4) Band

Line	Frequency	Δ_{hyp}	$\Delta_{\text{o-c}}$
P16	474408710.9	486.6	-0.7
P23	474319769.6	487.1	-0.5
P28	474239658.3	487.2	0.0
P34	474125274.3	487.3	-0.3
P42	473941774.0	487.4	0.2
P48	473780887.7	487.4	0.9
P52	473662541.6	487.4	-0.6
P56	473535320.4	487.5	-0.7
P60	473399216.6	487.5	-0.8
P62	473327831.5	487.5	-0.8
P78	472676623.2	487.5	-0.4
P80	472585190.1	487.5	-0.2
P81	472538636.2	487.5	0.0
P83	472443852.7	487.5	0.3
P84	472395622.4	487.5	0.0
P85	472346833.9	487.5	0.5
P91	472042351.2	487.5	-0.1
P95	471828162.3	487.5	0.7
P97	471717702.3	487.5	0.5
P102	471431725.5	487.5	0.0
P110	470944909.7	487.5	-0.4
P112	470817569.9	487.5	0.1
R22	474408682.6	487.0	-0.1
R29	474319699.8	487.2	-0.0
R34	474239541.1	487.3	0.0
R40	474125078.0	487.4	0.4
R50	473889963.3 ^a	487.4	1.1
R54	473780379.2	487.4	0.7
R56	473722254.3	487.4	0.5
R58	473661906.7	487.5	0.8
R61	473567213.9	487.5	0.1
R62	473534536.2	487.5	-1.0
R63	473501303.4	487.5	-0.6
R64	473467513.8	487.5	-0.4
R65	473433167.6	487.5	-0.1
R66	473398263.3	487.5	-0.9
R67	473362802.6	487.5	-1.0
R68	473326785.5	487.5	-0.4
R84	472674602.1	487.5	-0.3
R86	472583015.6	487.5	-0.1
R87	472536382.5	487.5	0.5
R89	472441433.1 ^a	487.5	-0.1
R90	472393118.1	487.5	0.5
R101	471824577.2	487.5	-0.2
R103	471713892.8	487.5	0.3
R105	471600952.8	487.5	-0.1
R108	471427311.7	487.5	-0.1

^a From Ref. (11).

They analyzed a large number of hyperfine splittings over a wide range of ν and J values, resulting in accurate hyperfine parameters. For both the X and B states the hyperfine constants can be represented by a power series in ν and J (7):

TABLE 6
Data for the (7, 3) Band

Line	Frequency	Δ_{hyp}	$\Delta_{\text{o-c}}$
P10	477359194.9	485.7	-0.4
P11	477351487.3	486.1	-0.2
P15	477315165.6	486.9	0.1
P17	477293709.7	487.1	-0.7
P18	477282157.8	487.2	0.3
P19	477270057.1	487.3	0.9
P57	476402712.8	487.9	0.3
P58	476369147.0	487.9	0.2
P60	476300359.6	487.9	0.2
P61	476265137.0 ^a	488.0	-0.5
P76	475670469.4	488.0	-0.4
P78	475581769.8	488.0	-0.0
P82	475397715.0	488.0	-0.5
P83	475350314.8	488.0	0.2
P84	475302358.9	488.0	0.3
P85	475253846.6	488.0	-0.7
P86	475204780.5	488.0	0.1
P87	475155157.8	488.0	-0.1
P88	475104979.4	488.0	-0.1
P89	475054245.5	488.0	0.3
P91	474951107.6	488.0	-0.2
P92	474898704.3	488.0	-0.2
P93	474845744.1	488.0	-0.4
P94	474792228.1	488.0	0.5
P95	474738154.2	488.0	0.5
R63	476404347.8	487.9	0.6
R64	476370781.9	487.9	0.3
R65	476336663.0	487.9	0.3
R66	476301991.5	487.9	1.1
R67	476266764.6	487.9	0.1
R82	475671855.2	487.9	-0.6
R84	475583095.4	487.9	-0.3
R88	475398899.3	487.9	0.0
R89	475351458.8	488.0	0.5
R90	475303460.5	488.0	0.3
R91	475254904.9	488.0	0.0
R92	475205792.4	488.0	0.4
R93	475156120.5	488.0	-1.0
R94	475105892.7	488.0	-0.5
R100	474792798.2	488.0	0.2
R101	474738659.1	488.0	-0.3
R103	474628704.6	488.0	0.8
R116	473859332.1	488.0	-0.2

^a From Ref. (11).

TABLE 7
Data for the (9, 4) Band

Line	Frequency	Δ_{hyp}	$\Delta_{\text{o-c}}$
P24	477639485.6	486.6	0.2
P51	477017128.8	487.0	-0.8
P68	476413954.0	487.0	0.0
P69	476373373.5	487.0	0.2
P70	476332224.8	487.0	-0.4
P76	476073411.3	487.0	0.2
P78	475982592.8	487.0	-0.3
P91	475336752.0	487.0	0.3
P92	475283078.0	487.0	-0.5
P93	475228833.2	487.1	-0.7
P94	475174018.6	487.1	0.8
P95	475118629.7	487.1	-0.2
P96	475062670.3 ^a	487.1	0.2
P97	475006138.1	487.1	0.0
P98	474949033.8	487.1	0.2
P99	474891357.1	487.1	0.5
P100	474833107.8	487.1	1.0
P102	474714888.1	487.1	0.3
P103	474654918.3	487.1	0.1
P104	474594376.1	487.1	1.2
P120	473547468.0	487.1	0.4
R15	477806665.2	486.0	0.4
R22	477743314.7	486.5	0.1
R23	477732011.1	486.6	-0.1
R26	477694720.3	486.7	0.4
R39	477474480.0	486.9	0.2
R48	477266117.0 ^a	486.9	-0.2
R50	477213595.8	487.0	-0.5
R55	477072391.9	487.0	-0.4
R57	477011947.3	487.0	-0.1
R67	476675708.3	487.0	-0.0
R74	476406557.1	487.0	0.4
R76	476324537.1	487.0	-0.2
R77	476282674.1	487.0	0.5
R80	476153666.0	487.0	1.4
R83	476019524.6	487.0	-0.3
R96	475378840.4 ^a	487.0	-0.0
R97	475325549.7	487.0	-0.4
R98	475271686.1	487.0	-0.2
R99	475217248.4	487.0	-0.4
R100	475162236.6	487.0	-0.7
R101	475106650.9	487.0	-0.8
R102	475050491.5	487.0	-0.2
R103	474993757.2	487.0	0.0
R104	474936447.9	487.0	0.2
R105	474878564.0	487.0	0.8
R107	474761066.2	487.0	-1.6
R108	474701455.9	487.0	-0.7
R109	474641268.3	487.0	-0.9
R121	473873993.9	487.0	0.2
R122	473806293.7	487.0	0.1

^a From Ref. (11).

$$eQq_X = -2452.3281 - 0.533(\nu + \frac{1}{2}) - 2.22 \times 10^{-4}J(J + 1) + 4.519 \times 10^{-2}(\nu + \frac{1}{2})^2 + 6.58 \times 10^{-6}(\nu + \frac{1}{2})J(J + 1) \quad [2]$$

and

$$eQq_B = -487.806 - 1.8644(\nu + \frac{1}{2}) - 1.66 \times 10^{-4}J(J + 1) - 2.08 \times 10^{-6}(\nu + \frac{1}{2})J(J + 1) - 2.47 \times 10^{-10}J^2(J + 1)^2. \quad [3]$$

TABLE 8
Data for the (10, 4) Band

Line	Frequency	Δ_{hyp}	$\Delta_{\text{o-c}}$
P25	480907213.8	486.2	-0.5
P31	480799303.3	486.4	0.9
P40	480598660.8	486.5	-0.1
P43	480521432.3	486.5	-0.6
P78	479237086.0	486.6	-0.1
P81	479094036.9	486.6	-0.6
P85	478895179.7	486.6	0.7
P89	478687021.4	486.6	-0.1
P91	478579451.8	486.6	0.2
P93	478469552.5	486.6	0.4
P97	478242757.8	486.6	0.0
P101	478006624.3	486.6	-0.0
P103	477885050.3	486.6	-0.6
R17	481076204.0	485.7	-0.1
R22	481027019.3	486.1	-0.2
R25	480990619.5	486.2	-0.4
R29	480934046.7	486.3	0.0
R34	480850402.7	486.4	0.6
R36	480812920.3 ^a	486.4	0.0
R39	480752384.0	486.4	-0.0
R42	480686669.6	486.5	0.3
R82	479314092.3	486.6	0.1
R85	479173774.6	486.6	-0.1
R89	478978533.1	486.6	-0.4
R91	478877415.6 ^a	486.6	-0.1
R92	478825981.8	486.6	0.1
R93	478773964.1	486.6	-0.0
R97	478560052.7	486.6	0.0
R104	478163183.5	486.6	0.2
R107	477984303.8	486.6	0.4
R109	477862114.2	486.6	0.0
R117	477349821.1	486.6	-0.2

^a From Ref. (11).

TABLE 9
Data for the (9, 3) Band

Line	Frequency	Δ_{hyp}	$\Delta_{\text{o-c}}$
P18	484004252.9	486.3	1.8
P24	483920855.1	486.6	-0.5
P40	483598068.8	486.9	1.6
P42	483547441.4	486.9	-0.4
P48	483381848.1	486.9	0.1
P70	482598319.5	487.0	-0.5
P74	482426019.8	487.0	-0.3
P75	482381507.3a	487.0	-0.1
P76	482336419.1	487.0	-0.1
P92	481536616.0	487.0	0.5
P93	481481719.4	487.0	0.3
P106	480715332.3	487.0	0.4
P107	480652315.5	487.0	0.5
R13	484102525.5	485.6	-1.0
R14	484096193.9	485.7	-0.5
R17	484073777.1	486.2	-0.9
R24	484001514.0	486.6	-0.6
R30	483917324.2	486.7	-0.1
R47	483567114.7a	486.9	0.4
R48	483541366.6	486.9	-0.1
R54	483374855.1	486.9	0.2
R76	482587545.2	487.0	-0.3
R80	482414473.9	487.0	-0.4
R81	482369763.9	487.0	-0.2
R82	482324477.1	487.0	0.4
R98	481521205.6	487.0	0.2
R100	481410360.7	487.0	0.2
R103	481239733.4a	487.0	0.1
R104	481181692.7	487.0	-1.3
R110	480821223.5	487.0	-0.1

^a From Ref. (11).

The above expressions give the quadrupole constants in megahertz. For the spin-rotation hyperfine constants C_X and C_B accurate formulae have been developed (7). For the present work, requiring an accuracy of hyperfine splittings of 0.2 MHz, it is sufficient to fix the value for the C constant in the electronic ground state: $C_X = 3.162$ kHz. For the $B(^3\Pi_u^+)$ state we adopt the expression

$$C_B = 2.93 - \frac{73913.6}{E(\nu_B) - 19684.6} \quad [4]$$

neglecting terms representing dependencies on J and ν and C_B in kilohertz (7); the energy $E(\nu_B)$ of the vibronically excited $B(^3\Pi_u^+)$, ν_B state must be given in reciprocal centimeters. With

these constants the shifts from center-of-gravity for the t -hyperfine components are calculated for all the measured transitions listed in Tables 1–15. The derived shifts Δ_{hyp} are included in these tables.

The values for the center-of-gravity frequencies represent the rovibronic structure of the I_2 molecule in the $B-X$ system. In an analysis of this structure we adopt the following energy representations for the $X^1\Sigma_g^+$, ν'' ground and $B^3\Pi_u^+$, ν' excited state:

$$E_{X\nu'} = E_{\nu''} + B_{\nu''}J(J+1) - D_{\nu''}J^2(J+1)^2 + H_{\nu''}J^3(J+1)^3 \quad [5]$$

$$E_{B\nu'} = E_{\nu''} + B_{\nu''}J(J+1) - D_{\nu''}J^2(J+1)^2 + H_{\nu''}J^3(J+1)^3 + L_{\nu''}J^4(J+1)^4. \quad [6]$$

These expressions are used in a least-squares optimization routine on the data for center-of-gravity frequencies separately for each band. Some of the values determined previously by other groups (8–11) (the ones listed in Tables 1–15) are

TABLE 10
Data for the (10, 3) Band

Line	Frequency	Δ_{hyp}	$\Delta_{\text{o-c}}$
P10	487369688.7	484.3	0.1
P17	487301350.0a	485.7	-0.4
P18	487289265.9	485.8	0.4
P20	487263353.4	486.0	-0.1
P36	486972396.2	486.4	0.9
P49	486626348.7	486.5	-0.3
P58	486329085.7	486.5	0.1
P71	485816176.6	486.5	0.4
P89	484942471.7	486.6	-0.8
P90	484888346.2	486.6	-1.6
P91	484833633.9a	486.6	-0.1
P92	484778331.2	486.6	0.7
P94	484665954.9	486.6	0.4
R17	487358600.4	485.7	-0.2
R18	487349786.0	485.8	0.1
R24	487284697.0	486.1	-0.4
R26	487258352.2	486.2	0.1
R42	486963828.0	486.4	0.9
R55	486614704.4	486.5	-0.4
R63	486350806.7	486.5	0.5
R76	485842039.1a	486.5	-0.5
R95	484919736.1	486.5	-0.7
R98	484754633.6	486.6	1.9
R110	484040850.7	486.6	-0.5

^a From Ref. (11).

TABLE 11
Data for the (11, 3) Band

Line	Frequency	Δ_{hyp}	$\Delta_{\text{o-c}}$
P22	490467731.3	485.6	0.5
P24	490436684.1	485.7	0.1
P46	489938814.1	486.0	2.2
P48	489879902.7 ^c	-96.7	-0.1
P76	488796584.0 ^a	486.1	-0.0
P77	488749266.9	486.1	-0.4
P80	488603728.0	486.1	-0.2
P96	487736395.8	486.1	0.4
P101	487433789.9	486.1	0.8
P103	487308524.7	486.1	-0.5
P105	487180844.5	486.1	-1.7
R13	490622030.6	484.7	-0.1
R28	490460079.1	485.8	0.6
R53	489893802.1	486.0	2.5
R76	489044383.3	486.1	1.3
R81	488817890.2	486.1	1.5
R82	488770791.5	486.1	-0.0
R86	488576400.9	486.1	-0.4
R96	488048335.1	486.1	0.1
R101	487761697.2	486.1	0.2
R110	487207642.3	486.1	-0.2
R111	487143050.2	486.1	0.6

^a From Ref. (11).

^c From Ref. (9).

included as well in the fitting routines. In our previous study it turned out that good convergence was obtained when the molecular constants for the ground state, $B_{v'}$, $D_{v'}$, and $H_{v'}$, are fixed to the values obtained by Gerstenkorn and Luc in the analysis of the Doppler-broadened spectrum (1). However for the present work we decided to take advantage of progress in the field, and now use the improved rotational analysis and the constants derived by the Hannover group. They developed a set of Dunham constants (7) from which we derive rotational constants for the electronic ground states. We list the constant used in our rotational analysis in Table 16. For the excited $B(^3\Pi_v^+)$ state we fix the constant representing the third-order centrifugal distortion $L_{v'}$ fixed at the value determined by Bodermann (7) of $3.86261 \times 10^{-21} \text{ cm}^{-1}$ for all vibrational bands.

The fitting routines are restricted to a band-by-band analysis. All the fits entail a four-parameter least-squares minimization routine varying $B_{v'}$, $D_{v'}$, $H_{v'}$, and ΔE . Since some excited vibrational levels are probed via various ground vibrational levels, a more refined procedure to extract molecular constants from the combined set of data is possible. However, the goal of

the present study is to deliver an accurate algorithm for predicting frequencies of t -hyperfine components and to generate a spectral atlas. The values for the parameters pertaining to the excited states are listed in Table 16. In view of the restricted fitting procedure band origins are given as $\Delta E = E_{v'} - E_{v''}$. Molecular constants are given in a number of decimals sufficient to obtain a nominal accuracy of 0.2 MHz. We note that the χ^2 value in each least-squares minimization routine is less than one per data point. This demonstrates the consistency of the procedures followed and it shows that the 1σ uncertainty adopted is not too low. The latter conclusion can also be drawn from the stated deviations between observed and calculated values as listed in Tables 1–15.

4. CONCLUSION: THE REFERENCE STANDARD

In the present analysis of hyperfine structure and rotational structure of 15 bands in the unperturbed spectrum of the $B-X$

TABLE 12
Data for the (12, 3) Band

Line	Frequency	Δ_{hyp}	$\Delta_{\text{o-c}}$
P11	493778516.6	483.8	-0.3
P14	493750182.2	484.5	-0.0
P16	493728280.1	484.8	-0.1
P41	493251010.2	485.5	-0.6
P62	492558263.7	485.6	-0.6
P68	492311233.6	485.7	0.0
P78	491850864.9	485.7	0.1
P81	491700872.7	485.7	-0.0
P82	491649654.8	485.7	-0.1
P85	491492336.9	485.7	-0.3
P88	491329518.9	485.7	0.5
P98	490746978.3	485.7	-0.9
P103	490432686.8	485.7	-0.1
P105	490302662.3	485.7	0.3
R17	493772909.4	484.8	0.5
R19	493753844.0	485.0	0.1
R22	493720724.9	485.2	0.3
R24	493695629.6	485.3	-0.2
R50	493149584.9	485.6	0.2
R51	493120417.9	485.6	0.4
R68	492531739.3	485.6	-0.1
R73	492325157.9	485.6	0.2
R83	491866244.0	485.7	0.4
R85	491767126.4	485.7	0.0
R90	491508614.8	485.7	0.2
R94	491290764.3	485.7	-0.1
R104	490703087.2	485.7	-0.2
R111	490255003.5	485.7	0.1

TABLE 13
Data for the (11, 2) Band

Line	Frequency	Δ_{hyp}	$\Delta_{\text{o-c}}$
P16	496866466.2	485.1	-1.3
P22	496786713.8	485.6	-0.8
P24	496755340.7 ^a	485.6	-0.9
P27	496703790.6 ^a	485.7	-0.3
P32	496605893.3	485.8	-0.1
P36	496516788.3	485.9	-0.6
P49	496161498.1 ^b	-96.7	-0.1
P56	495927247.1	486.0	1.0
P65	495583483.7	486.0	0.0
P68	495458047.6	486.0	-0.0
P72	495282350.4	486.0	0.2
P76	495096987.8	486.0	1.4
P77	495049134.9	486.0	1.1
P83	494749304.8	486.0	-0.7
R9	496963160.7	483.1	-1.0
R9	496963234.0 ^b	411.0	0.2
R25	496821608.4	485.7	-0.3
R28	496778000.5	485.7	0.5
R29	496762264.9	485.7	-0.4
R32	496711463.7	485.8	-0.3
R34	496674599.0	485.8	0.4
R40	496549603.6 ^b	485.8	0.1
R44	496454267.4	485.9	0.5
R46	496402994.3	485.9	0.1
R56	496110547.5	486.0	0.2
R58	496044834.3	486.0	0.2
R65	495795846.8	486.0	0.5
R73	495475642.6 ^b	-96.9	-0.1
R76	495344784.9	486.0	0.3
R79	495209036.1 ^b	507.5	-0.0
R80	495162602.9 ^b	486.0	0.0
R96	494336687.3	486.1	-0.1
R103	493926282.7	486.1	-0.5
R110	493485886.9	486.1	0.3
R111	493420518.8	486.1	-0.0

^a From Ref. (11).

^b From Ref. (8); various components used.

system of I₂, a representation is found for the hyperfine components in the spectrum. The rotational analysis, using fixed values for the ground state (listed in Table 16) and fitted values for the excited state (listed in Table 17), yields a representation accurate to within 1 MHz for all rotational lines up to $J = 120$. The hyperfine structure is known to much higher precision and with the presently used approximations still is good to within 0.2 MHz. Hence all t -components can be predicted from the defined parameter space to within 1 MHz with a 1σ uncertainty. Calculated values for these t -components are listed in

the appendix to this paper (to be found in the database of the Journal of Molecular Spectroscopy) for all P and R transitions from $J = 9$ to 120 for the 15 bands delivering roughly 3400 reference lines. In all bands the rotational fits include values up to $J = 110$, while in several bands values up to $J = 120$ were obtained. In the latter cases inclusion of the highest J values does not induce a significant shift in the parameters. For this reason it is justified to allow for some extrapolation to $J = 120$ in some bands. Since the 15 bands are chosen to overlap, the entire wavelength range 595–655 nm is covered with a refer-

TABLE 14
Data for the (12, 2) Band

Line	Frequency	Δ_{hyp}	$\Delta_{\text{o-c}}$
P13	500080338.2	484.3	-0.2
P16	500048076.4	484.7	-0.4
P30	499824973.4	485.4	0.4
P34	499739267.2	485.4	-0.2
P64	498784637.9	485.6	-0.5
P67	498658835.1	485.6	-0.1
P72	498436867.9	485.6	1.0
P73	498390626.8	485.6	-0.3
P75	498296299.8	485.6	-0.3
P79	498100250.5	485.6	-0.2
P80	498049696.2	485.6	-0.2
P101	496845150.9	485.6	1.2
P103	496716159.0	485.6	1.0
P114	495962116.7 ^b	485.7	0.0
R9	500145490.3	482.6	0.4
R16	500101333.5	484.7	-0.2
R17	500092587.4	484.8	-0.0
R31	499906091.3	485.4	1.0
R40	499723004.4	485.5	0.4
R50	499461469.7	485.5	-0.2
R60	499138651.9	485.6	-1.5
R69	498795599.4	485.6	0.2
R71	498712594.9	485.6	-0.1
R74	498583466.5	485.6	0.3
R75	498539190.6	485.6	0.8
R78	498402657.7 ^a	485.6	0.2
R79	498355911.9	485.6	0.2
R88	497907366.3	485.6	-0.1
R95	497523787.1	485.6	-0.2
R100	497231153.8	485.6	-0.6
R103	497048098.1	485.6	-1.2
R105	496922943.0	485.6	-0.2
R106	496859428.3	485.6	0.0
R107	496795288.6	485.6	-0.1
R108	496730523.8	485.6	-0.0

^a From Ref. (11).

^b From Ref. (8).

TABLE 15
Data for the (13, 2) Band

Line	Frequency	Δ_{hyp}	$\Delta_{\text{o-c}}$
P10	503236697.8	483.0	-1.3
P12	503219219.7	483.6	-0.4
P13	503209549.5	483.8	-0.1
P16	503176814.7	484.3	0.5
P24	503062202.3	484.8	0.2
P29	502970382.7	484.9	0.0
P45	502572092.7	485.1	0.8
P53	502313160.9	485.1	1.5
P60	502053831.6	485.1	0.9
P74	501443217.6	485.2	0.4
P84	500931771.1	485.2	0.9
P93	500417619.8	485.2	0.9
P96	500234866.6a	485.2	0.3
P97	500172683.4	485.2	0.0
P99	500046418.3	485.2	0.7
P112	499163796.1	485.2	1.2
P114	499018459.9	485.2	1.4
R16	503229697.7	484.2	-1.2
R22	503166686.7	484.7	0.7
R34	502973539.7	485.0	0.9
R49	502606053.3	485.1	1.0
R52	502515717.4a	485.1	0.2
R55	502419760.9	485.1	0.1
R60	502247330.6	485.1	0.2
R66	502019757.8b	485.1	-0.1
R103	500115824.1	485.2	-1.2
R107	499858077.5	485.2	-0.4
R110	499658074.0	485.2	-1.1
R111	499590129.6	485.2	-1.4

^a From Ref. (11).

^b From Ref. (8).

ence line per reciprocal centimeter. This density is required since most scanning laser systems of the highest resolution only allow for single continuous scans of a wavenumber. Combined with our previous work (3), the range 571–655 nm

TABLE 17

Values for the Rotational Constants of the $B^3\Pi_u^+$, ν' States Resulting from the Fitting Routines

(ν', ν'') Band	ΔE	$B_{\nu'} \times 10^2$	$D_{\nu'} \times 10^9$	$H_{\nu'} \times 10^{15}$
(6,5)	15391.975104	2.79760924	7.002995	3.8216
(5,4)	15484.026909	2.81411084	6.854413	3.6535
(6,4)	15600.317449	2.79760997	7.002539	3.8904
(7,4)	15714.974653	2.78081698	7.157694	4.3791
(8,4)	15827.977714	2.76371510	7.318009	4.9491
(7,3)	15924.568525	2.78081923	7.161795	4.1843
(9,4)	15939.305205	2.74630436	7.498425	5.1286
(10,4)	16048.935801	2.72856017	7.680300	5.7368
(9,3)	16148.899020	2.74630699	7.501372	5.0240
(10,3)	16258.529629	2.72856115	7.677110	6.1169
(11,3)	16366.441532	2.71047851	7.876606	6.2559
(12,3)	16472.612832	2.69204267	8.085218	6.7762
(11,2)	16577.278739	2.71047948	7.875540	6.3736
(12,2)	16683.450044	2.69204551	8.090124	6.5010
(13,2)	16787.858615	2.67324253	8.307612	7.3009

Note. $L_{\nu'}$ is fixed at $3.86261 \times 10^{-21} \text{ cm}^{-1}$. All values in cm^{-1} .

is now covered with a dense grid of reference lines that may provide a useful spectral atlas for future research. A remark of caution deals with the interaction between the $B^3\Pi(0_u^+)$ state and the repulsive $^1\Pi_{1u}$ state, causing predissociation in the B state and possibly shifts in the rovibrational structure (14), particularly in the range where the interaction is strongest, near $\nu' = 5-6$. In the interaction with a continuum state the shifts are global, slowly varying over the J -quantum number; hence, the perturbation is included in the set of parameters describing the B state. No marked deviations in the rotational structure are found as an indication of the perturbation.

The presently obtained data can be included in a highly accurate description of the $B-X$ system in terms of a Dunham or a potential representation for both ground and excited states. Bodermann (7) embarked on such a project taking all data of well-calibrated I_2 -saturation lines available in the literature, including the ones of our previous study (3), in the input set. Based on this analysis, a prediction can be made for the absolute frequency of any hyperfine component in a rovibrational band in the $B-X$ system. We verified for two bands that predictions for the frequencies of the t -components for all J values are within 5 MHz of the presently measured values. This demonstrates the usefulness of such an analysis; the entire I_2 -absorption spectrum can now be predicted to within this accuracy; undoubtedly inclusion of the presently measured 481 additional lines will improve the accuracy of the representation, and possibly the entire spectrum ranging from 500 to 900 nm can in the future be predicted to within 1 MHz. As an intermediate step we restricted ourselves to the band-by-band analysis pertaining to a limited range; in the range 595–655 nm a secondary frequency standard of 1 MHz accuracy is established.

TABLE 16
Values for the Rotational Constants of the $X^1\Sigma_g^+$, ν'' Ground State Used in the Fitting Routines

ν''	2	3	4	5
$B_{\nu''} \times 10^2$	3.70817246	3.69659312	3.68494715	3.67323219
$D_{\nu''} \times 10^9$	4.5887580	4.6133781	4.6393651	4.6667191
$H_{\nu''} \times 10^{16}$	7.02303	7.43833	7.85364	8.26894

Note. Values in cm^{-1} .

ACKNOWLEDGMENTS

The authors thank I. Velchev for assistance during the measurements and H. Knöckel and the other members of the Hannover group for fruitful discussions, for sending us their results prior to publication, and for providing a computer program to verify calculations on the hyperfine structure.

REFERENCES

1. S. Gerstenkorn and P. Luc, "Atlas du spectre d'absorption de la molecule de l'iode entre 14800–20000 cm^{-1} ," Presses du CNRS, Paris, 1985. [We use the 1985 version with the "Complément" containing line identifications and details on the rotational analysis.]
2. S. Gerstenkorn, J. Verges, and J. Chevillard, "Atlas du spectre d'absorption de la molecule de l'iode entre 11000–14000 cm^{-1} ," Presses du CNRS, Paris, 1982.
3. I. Velchev, R. van Dierendonck, W. Hogervorst, and W. Ubachs, *J. Mol. Spectrosc.* **187**, 21–27 (1998).
4. H. Knöckel, S. Kremser, B. Bodermann, and E. Tiemann, *Z. Phys. D: At. Mol. Clusters* **37**, 43–48 (1996).
5. B. Bodermann, G. Bönsch, H. Knöckel, A. Nicolaus, and E. Tiemann, *Metrologia* **35**, 105–113 (1998).
6. B. Bodermann, M. Klug, H. Knöckel, E. Tiemann, T. Trebst, and H. R. Telle, *Appl. Phys. B* **67**, 95–99 (1998).
7. B. Bodermann, PhD thesis, University of Hannover, 1998.
8. D. Shiner, J. M. Gilligan, B. M. Cook, and W. Lichten, *Phys. Rev. A: Gen. Phys.* **47**, 4042–4045 (1993).
9. T. J. Quinn, *Metrologia* **30**, 523–541 (1993).
10. C. S. Edwards, G. P. Barwood, P. Gill, F. Rodríguez-Llorente, and W. R. C. Rowley, *Opt. Commun.* **132**, 94–100 (1996).
11. C. J. Sansonetti, *J. Opt. Soc. Am. B: Opt. Phys.* **14**, 1913–1920 (1997).
12. G. R. Hanes, J. Lapierre, P. R. Bunker, and K. C. Shotton, *J. Mol. Spectrosc.* **39**, 506–515 (1971).
13. Ch. J. Bordé, G. Camy, B. Decomps, J. P. Descoubes, and J. Vigué, *J. Phys.* **42**, 1393–1411 (1981).
14. J. Vigué, M. Broyer, and J. C. Lehmann, *J. Phys.* **42**, 937–948 (1981); *J. Phys.* **42**, 961–978 (1981).